Scientific Research and Essays Vol. 6(17), pp. 3702-3716, 26 August, 2011
Available online at http://www.academicjournals.org/SRE
DOI: 10.5897/SRE11.616
ISSN 1992-2248 ©2011 Academic Journals

Full Length Research Paper

The effect of welding parameters on the mechanical and microstructural properties of friction stir welded dissimilar AA 3003-H24 and 2124/SiC/25p-T4 alloy joints

Yahya BOZKURT[1]* and Serdal DUMAN[2]

[1]Department of MaterialsTechnology, Technical EducationFaculty, Marmara University, 34722, Göztepe - Istanbul / Turkey.
[2]Department of MaterialsTechnology, Institute For Graduate Studies in Pure and Applied Sciences, Marmara University, 34722, Göztepe - Istanbul/Turkey.

Accepted 18 July, 2011

Assemblies consisting of aluminum and particle reinforced aluminum composite alloys have wide spread applications in construction and automotive industries. For a successful use of such dissimilar joints, the welds must have sufficient strength and formability. In the present study, 3003-H24 aluminum alloy and 2124/SiC/25p-T4 composite plates were successfully friction stir butt joined by offsetting the high strength plate to retreating side of the tool under tool rotational speed of 900 to 1400 rpm and traversing speed of 40 to 125 mm/min, keeping other parameters constant. Ultimate tensile strength, percentage elongation and joint efficiency values of the welded joints and hardness variations across the weld interface were determined. The integrity of the joints was investigated using optical microscopy, scanning electron microscopy and energy dispersive spectroscopy. Results indicated that the high quality welded joints could be obtained when a tool rotational speed of 900 rpm and a traverse speed of 125 mm/min were employed. The maximum tensile strength value obtained was about 182 MPa, which corresponds to a joint efficiency of 104% of that of the aluminum alloy base metal.

Key words: Friction stir welding, dissimilar joint, microhardness, mechanical properties.

INTRODUCTION

Aluminum based metal matrix composites (Al-MMCs) possess improved specific stiffness and strength-to-weight ratio at room and elevated temperatures, excellent fatigue properties, high formability and improved wear resistance, and greater thermal stability in respect to the corresponding unreinforced matrix alloys, thus finding applications mainly in the aerospace, automotive and motorsport fields (Uzun, 2007; Rotundo et al., 2010). Similarly, aluminum and its alloys are important metallic materials used in various areas. Due to its low cost, high specific strength, high thermal conductivity as well as good corrosion resistance, 3003 Al alloy has been widely used for automotive heat exchangers to replace more traditional materials like stainless steels and copper alloys (Mei-jun et al., 2010). Joining of these dissimilar materials is becoming increasingly important in industrial applications due to their numerous advantages. These include not only technical advantages, such as desired product properties, but also benefits in terms of production economics. Therefore, the existence of suitable joining techniques for dissimilar materials is indispensable. However, dissimilar metals are difficult to be joined with conventional fusion welding methods due to their different chemical and physical characteristics, thus solid state joining methods have received much attention in recent years (Xue et al., 2010). The conventional fusion welding of aluminum and its alloys

*Corresponding author. E-mail: ybozkurt@marmara.edu.tr. Tel: +90 216 336 57 70/357. Fax: +90 216 337 89 87.

Table 1. The chemical composition of AA 3003-H24 and AA2124/SiC/25p-T4 MMCs plates (mass %).

Material	Cu	Mg	Mn	Si	Fe	Al
AA2124/SiC/25p-T4	3.86	1.52	0.65	0.17	-	93.8
AA3003-H24	0.05	0.12	1.20	0.15	0.46	98.02

has always been a great challenge for designers and technologists. The difficulties associated with fusion joining are mainly related to the presence of a tenacious oxide layer, high thermal conductivity, high coefficient of thermal expansion, solidification shrinkage and high solubility of hydrogen and other gases in molten state. The fusion welding of aluminum alloys leads to the melting and re-solidification of the fusion zone which results in the formation of brittle inter-dendritic structure and eutectic phases. The formation of brittle structures in the weld zone leads to a drastic decrease in the mechanical properties, such as in hardness, strength and ductility (Shanmuga and Murugan, 2010; Çam et al., 1999, 2000; Çam and Koçak, 2007) in fusion welding processes. These problems are not encountered in friction stir welding because it is a solid-state process where the maximum process temperature does not reach the melting point of the welded materials (Leal and Loureir, 2008).

Wert (2003) and Sharifitabar and Nami (2011) observed formation of grain boundary films during dissimilar friction stir welding of 2024 to 2014 AA reinforced with 20 vol% particulate Al_2O_3 and 2024 aluminum alloy to Al/Mg_2Si metal matrix cast composite, respectively. Wert stated that overheating may be attributed to the unusually high tool rotation rate used in the dissimilar welds for the purpose of adequately softening of two base materials. In addition, the heat input from friction/plastic deformation increases with increasing flow stress. He concluded that because the flow stress of the MMC is higher than that of the monolithic alloy, the heat input for the welds is likely to be higher than in the case of two monolithic 2024 aluminum alloy plates welded using the same conditions. Both factors favor higher temperatures in the dissimilar 2024AA to 2014 AA/Al_2O_3 composite weld. So, in FSW of dissimilar welds, some liquid metal may forms in some situations. Friction stir welding (FSW) patented in 1991 by the Welding Institute in the United Kingdom (Liu et al., 2009), has several advantages such as a lower welding temperature and shorter welding time than conventional welding methods. Therefore, FSW is potentially a practicable joining process for dissimilar materials (Tanaka, 2009a). In FSW, a rotating tool is fed through the joint between the two plates to be welded. The tool rotation promotes mechanical (solid-state) mixing of the materials on the advancing and retreating sides of the weld. In this process, joining of the materials is facilitated by severe plastic deformation in the solid state, involving dynamic recrystallization of the base material (Somasekharan and Murr, 2004). Recently, some reports have been available on the friction stir welding of dissimilar alloys by FSW, such as joining of different Al alloys (Shigematsu et al., 2003; Wert, 2003; Ghosh et al., 2010; Khodir and Shibayanagi, 2008; Cavaliere et al., 2009a), aluminum to steel (Chen and Kovacevic, 2004; Tanaka, 2009a), Ti and aluminum to stainless steel (Najafabadi et al., 2010; Uzun, 2005), aluminum to magnesium (Yong et al., 2010), aluminum to copper (Liu et al., 2008), copper to brass alloy (Barlas and Uzun, 2010). However, a study on dissimilar joining of AA3003-H24 to AA2124 containing 25 vol% SiC particles reinforcement metal matrix composite (AA2124/SiC/25p-T4 MMC) by FSW has not been reported to date.

In the present study, these dissimilar two plates were joined successfully by FSW. The mechanical properties and microstructural evolutions in the dissimilar Al/MMCs joints obtained by employing different parameters were determined. The results obtained provide an important fundamental for further studying of FSW Al/MMCs dissimilar materials.

MATERIALS AND METHODS

The cold rolled 3003 aluminum alloy produced by ASSAN (TR) and AA2124/SiC/25p MMC plates produced by Aerospace Metal Composites Ltd (UK), with dimensions of 50 × 150 × 3 mm (3003 in H24 and 2124 in the T4 condition) were used in this study. The chemical compositions of the plates are given in Table 1. 3003-H24 Al alloy and AA2124/SiC/25p-T4 MMC were successfully butt joined by friction stir welding with different tool rotation speeds (900,1120 and 1400 rpm) and traverse speeds (40-80-125 mm/min) with a constant tilt angle of 2° which were chosen according to the optimum results obtained for AA2124/SiC/25p-T4 MMC plates (Bozkurt et al., 2011a). The dissimilar joints were produced with the high strength alloy (AA2124/SiC/25p-T4) positioned on the retreating side and the AA3003-H24 (the softer one) on the advancing side. This plate positioning was chosen based on the consideration that the microstructure and the mechanical properties of the stirred zone are influenced by the retreating side of the joint in order to obtain defect-free joints. Such dependence of the strength on the material position was previously observed for dissimilar AA6082/AA2024 (Cavaliere et al., 2009a) and AA6061/A356 alloys (Lee et al., 2003). The max. tensile properties were obtained for these joints with the high strength Al alloys positioned on retreating side of the weld. All the FSW trials were performed with an FSW-adapted universal milling machine. The FSW tool was made of high speed steel with shoulder diameter 20 mm, pin diameter 6 mm and cylindrical pin length 2.8 mm. Figure 1 shows the dissimilar FSW process. The rotating tool pin along with the shoulder during its travel produces frictional heat with

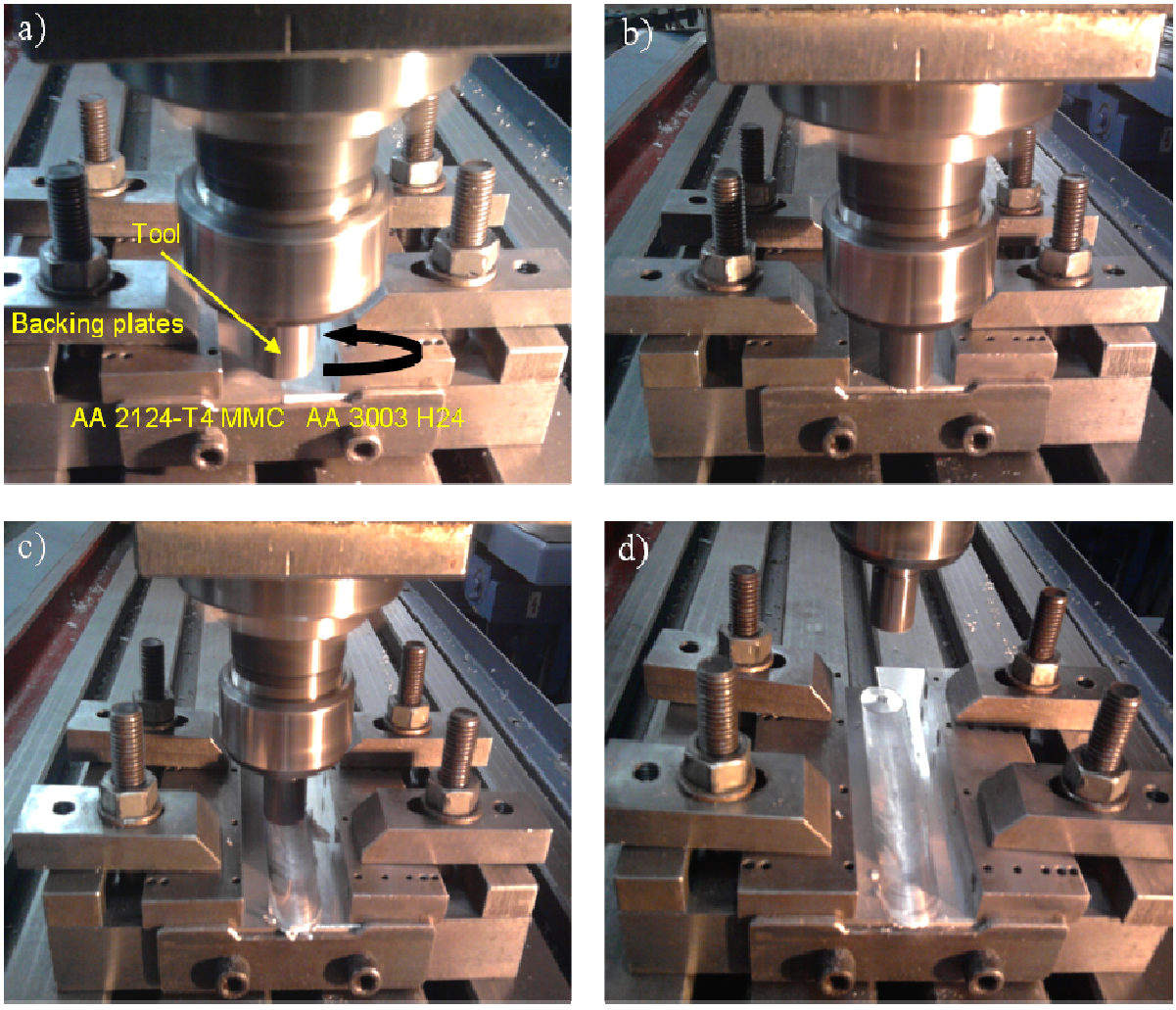

Figure 1. Dissimilar friction stir welding process: a) rotating tool prior to penetration into the butt joint; b) tool shoulder makes contact with the part, creating heat; c) restricting further penetration while expanding the hot zone and moving parts under the tool, creating a friction stir weld nugget; d) retraction of the tool from the joining zone.

temperature below the melting point and plastic deformation due to the stirring of the material around the pin, forming the weld (Gopalakrishnan and Murugan, 2011). After FSW process, the joints were sectioned perpendicular to the welding direction by wire electric discharge machining device for metallographic and mechanical investigations.

The welded specimens were polished with 9 and 1 µm diamond paste according to ASTM E3 (ASTM E3-01, 2007), standard and chemically etched with Keller's reagent. Microhardness ($HV_{0,5}$) tests were performed on the cross-sections of the welded joints both at the top and root locations with a 1 mm interval using 500 g load for 20 s to determine the hardness variations from base material to stir zone. The tensile tests were also carried out at room temperature according to ISO/TTA2 standard (ISO/TTA2, 1997) using universal type tensile test machine to determine the tensile properties of the joints. At least three specimens were tested under the same conditions to guarantee the reliability of the results. Microstructural and chemical analyses were performed from the cross-sections of FSWed joints by optical microscope (OM) and scanning electron microscope (SEM). The distributions of chemical elements in the stir zone were analyzed by energy dispersive X-ray spectroscopy (EDS) system.

RESULTS AND DISCUSSIONS

Appearances

In the present study, 3003-H24 Al alloy and AA2124/SiC/25p-T4 MMC plates were successfully butt-joined by the FSW. Although some prosity was formed in the weld area of the dissimilar joint produced at low transverse speed (that is 40 mm/min), the other joints exhibited no visible superficial defects, which are generally observed in the welded zone of the composite and Al joined using conventional fusion arc welding processes (such as porosity, reinforcement segregation

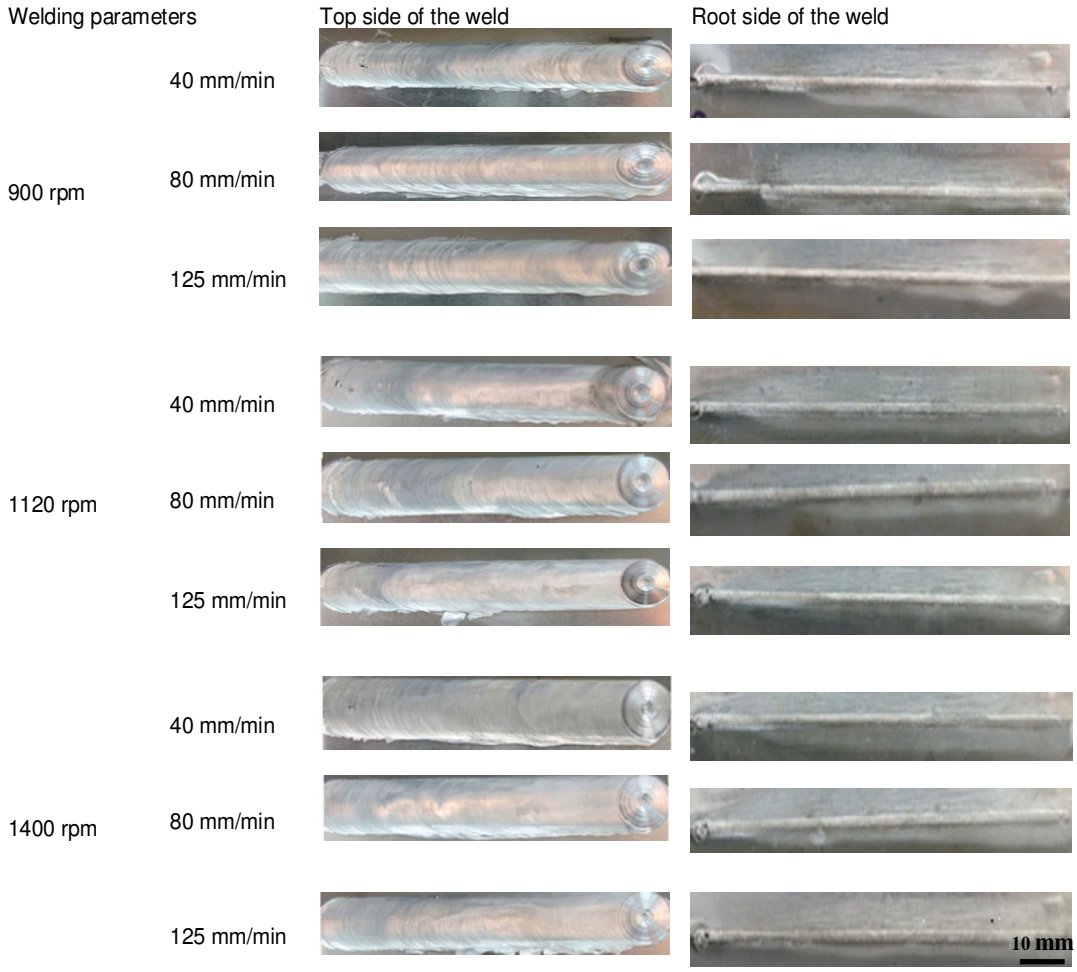

Figure 2. Top and root surfaces after FSW of dissimilar Al alloy and MMCs.

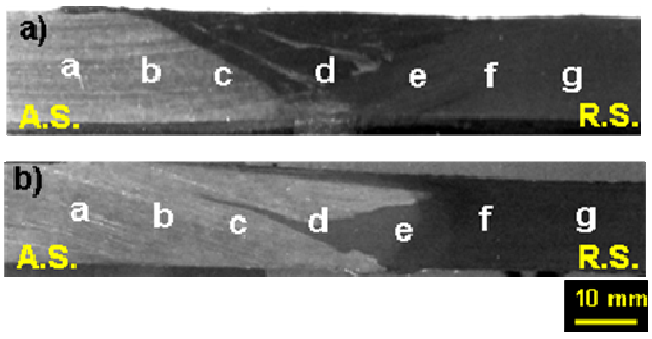

Figure 3. Macrographs of the Al/MMC cross-section of the FSW joints, (a) 900/125 and (b) 1400/40 welding parameters.

or carbide formation) (Ceschini et al., 2007a). In addition, the surface morphology of FSW zone became smoother with increasing tool transverse speed. Figure 2 shows the top and root surfaces after FSW of dissimilar Al alloy and MMCs with different tool rotation and welding speeds.

Microstructure

The macroscopic cross-sections of different welded zones are shown in Figure 3. In these cross-sections, typical features of the stir zones of dissimilar Al/MMC FSW joints are observed. The weld zone consists of several characteristic areas. All the dissimilar welds exhibit different microstructural zones from the other welding techniques (Sarsilmaz et al., 2010a) as shown in Figures 3a and b. Figure 3 shows the weld regions of two of the joints obtained, one exhibiting the highest mechanical properties (that is, 900 rpm tool rotation speed and 125 mm/min tool transverse speed: 900/125 rev/mm welding parameters) and the other displaying the lowest results (that is, 1400/40 welding parameters). Figures 4a and b shows the optical microscopy examination of the stir zones of the joints produced at 900/125 and 1400/40 weld parameters, respectively. It is interesting to note that the onion rings are clearly visible in the stir zones which is typically formed by the process of frictional heat due to rotation of the tool where the

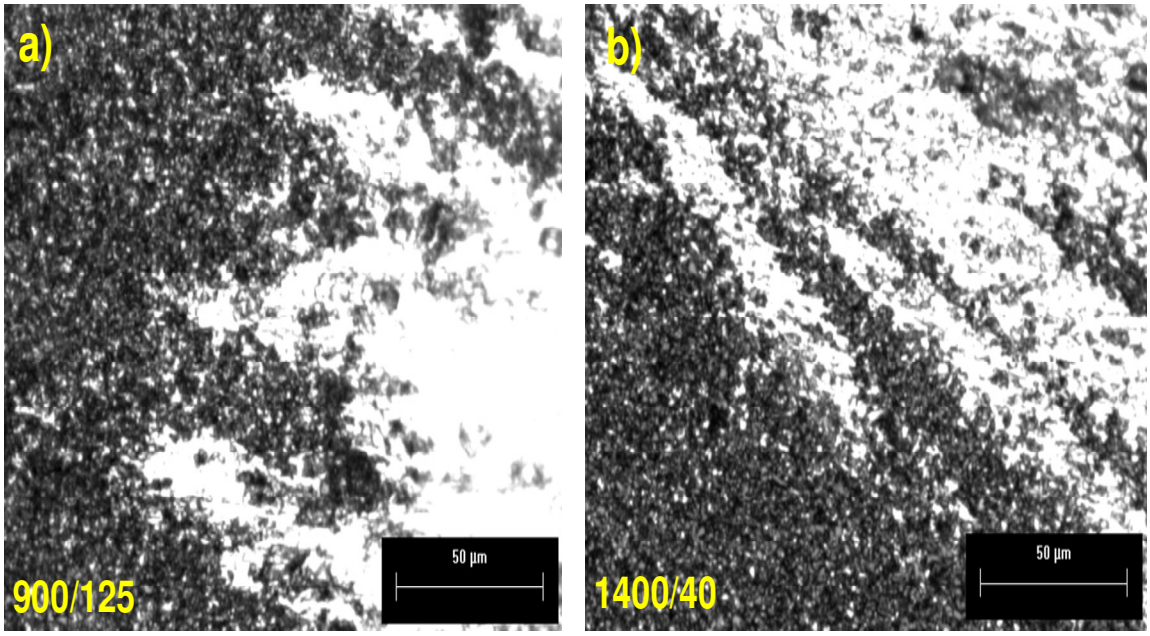

Figure 4. Microstructure of the stir zones (a), stir zone of 900/125, and (b) stir zone of 1400/40 welding parameters.

forward movement extrudes metal from advancing side (AS) to the retreating side (RS) of the tool. Other authors have reported a similar behaviour and related it to a partial recrystallization in the stirred zone (Ceschini et al., 2007b). Feng et al. (2008) found that the onion rings in the stir zone of the friction stir welded AA2009/SiCp composite included small particle rich-bands and large SiC particles did not segregate in the onion rings. Nami et al. (2011) showed that in frction stir welding of Al/Mg_2Si cast composite, onion rings in the stir zone consisted of alternating bands of needle shape eutectic Mg_2Si phase and Mg_2Si particles. There was no large Mg_2Si particle in the bands of one pass welded samples. Figures 5 and 6 show SEM micrographs of the dissimilar Al/MMC FSW joints produced at 900/125 and 1400/40 welding parameters at different locations of the joint. The microstucture of AA2124/SiC/25p-T4 BM, as shown in Figure 5g, consists of the AA2124 aluminum alloy matrix with an almost uniform distribution of coarse (<6 µm) and fine grained (<3 µm) silicon carbide particles (SiC_p) (Bozkurt et al., 2011a).

The stir zone which appeared to be composed of different regions of both the Aluminum and MMC alloys experienced the highest strain and undergoes recrystallization (Cavaliere et al., 2009a) exposure to high stresses and the heat produced by stirring tool is responsible for the plastic deformation which results in the rearrangement of the particles. Aluminum and SiC particles were homogeneously distributed in the stir zone and the microstructure of this zone was characterized fine equiaxed recrystallized grains (Bozkurt et al., 2011a) as shown in Figures 5d and 6e. This recrystallized microstructure is formed as a result of the mechanical action of the tool probe that generates a continuous dynamic recrystallization process. From this point of view, some researchers demonstrated that the microstructure in the stir zone evolves through a continuous dynamic recrystallization process (Cerri and Leo, 2010). The higher temperature and the severe plastic deformation during the weld in the stirred zone result in a recrystallized equiaxed grained structure with a grain size much finer than BM. Although tool wear took place in the similar butt joining of AA2124/SiC/25p-T4 MMC plates at the welding parameters of 900/100 causing the formation of Cu_2FeAl_7 phase (Bozkurt et al., 2011b), no evidence of porosity and particle cracking or tool wear was observed in the stir zones of dissimilar joints, (Figures 5d and 6e). TMAZ regions (Figures 5c and e, 6b and d), which are adjacent to the stir zone from both the advancing and the retreating sides, were also plastically deformed and thermally affected. The strong stirring effect can be advantageous on the homogeneity of the particles distribution. However, the TMAZ region of 3003-H24 Al alloy in the joint produced at 1400/40 welding parameters showed a non-uniform distribution of SiC particulates.

The HAZ (Figures 5b, f, 6a and c), between TMAZ and BM regions both at the advancing and retreating sides, exhibited a microstructure similar to the BM.

Microhardness of FSWed dissimilar Al/MMCs plates

The hardness profiles were evaluated by taking averages of both the top and root side of the FSW joints as shown

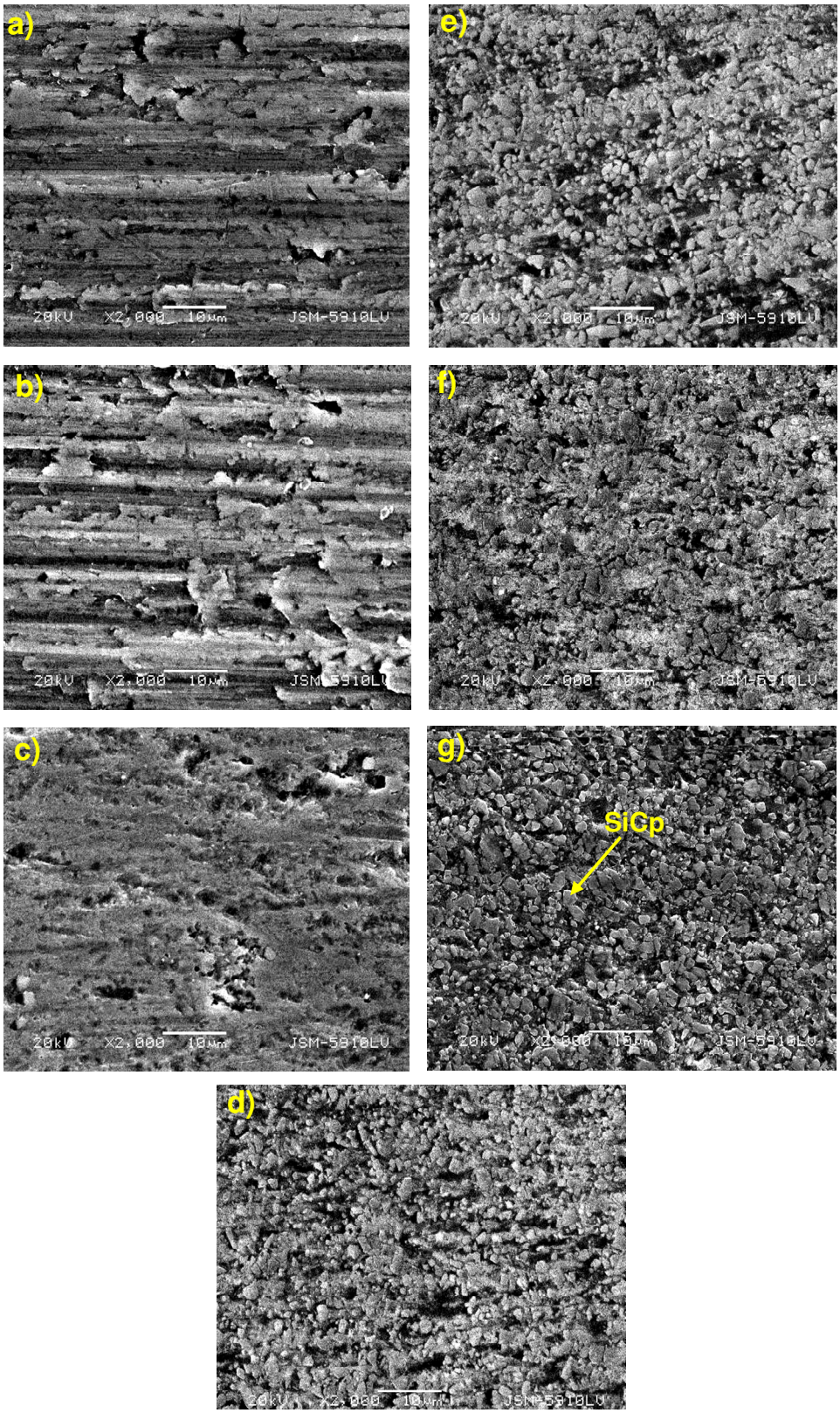

Figure 5. SEM micrographs of dissimilar FSWed plates at 900/125 welding parameters; a) AA3003-H24 BM, b) HAZ of AA3003-H24, c) TMAZ of AA3003-H24, d) stir zone for the AA3003-H24 and AA2124/SiC/25p-T4 MMC, e) TMAZ of AA2124/SiC/25p-T4 f) HAZ of AA2124/SiC/25p-T4 MMC and (g) AA2124/SiC/25p-T4 BM.

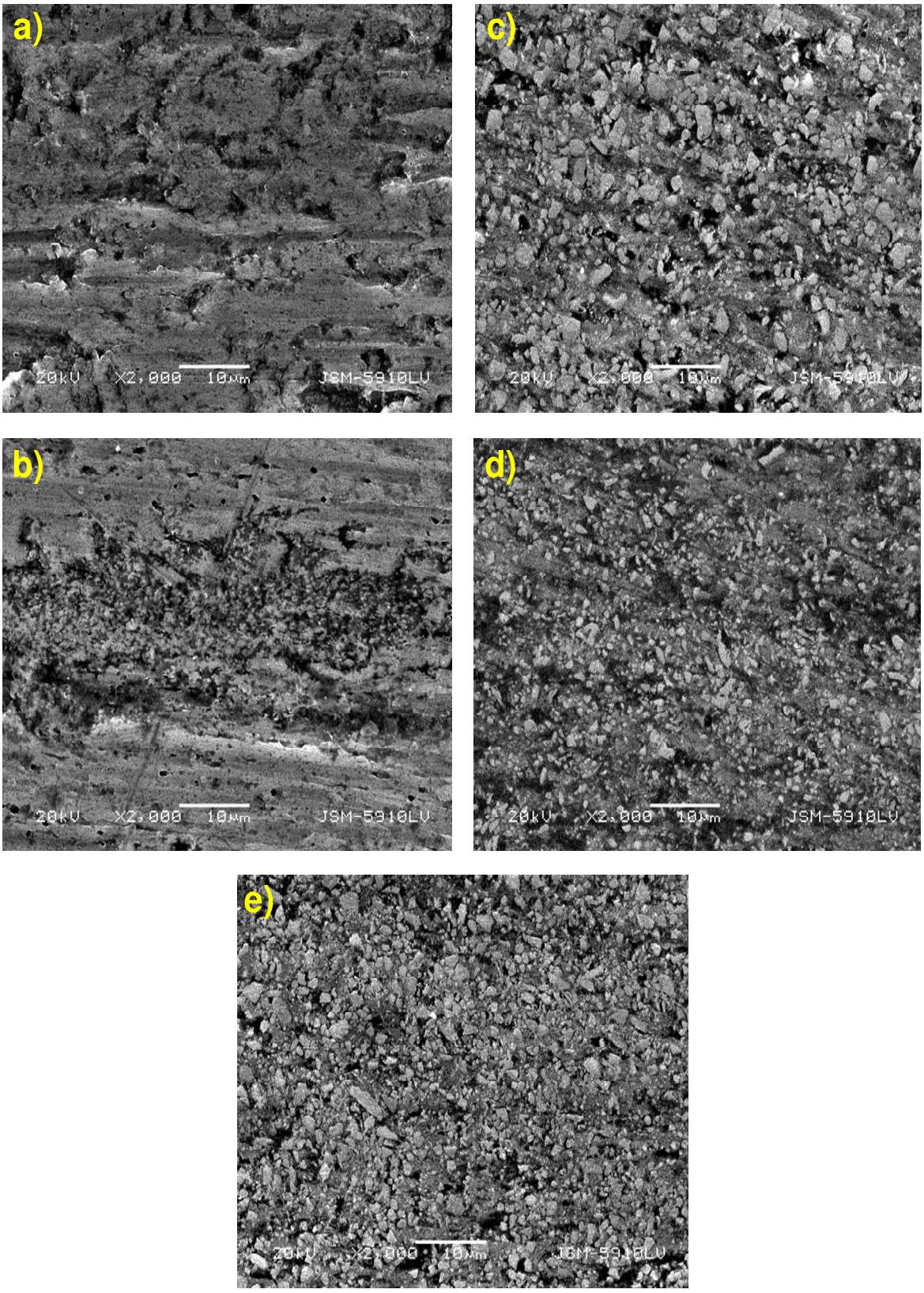

Figure 6. SEM micrographs of dissimilar FSWed plates at 1400/40 welding parameters; a) HAZ of AA3003-H24, b) TMAZ of AA3003-H24, c) HAZ of AA2124/SiC/25p-T4 MMC, d) TMAZ of AA2124/SiC/25p-T4, e) stir zone for the AA3003-H24 and AA2124/SiC/25p-T4 MMC.

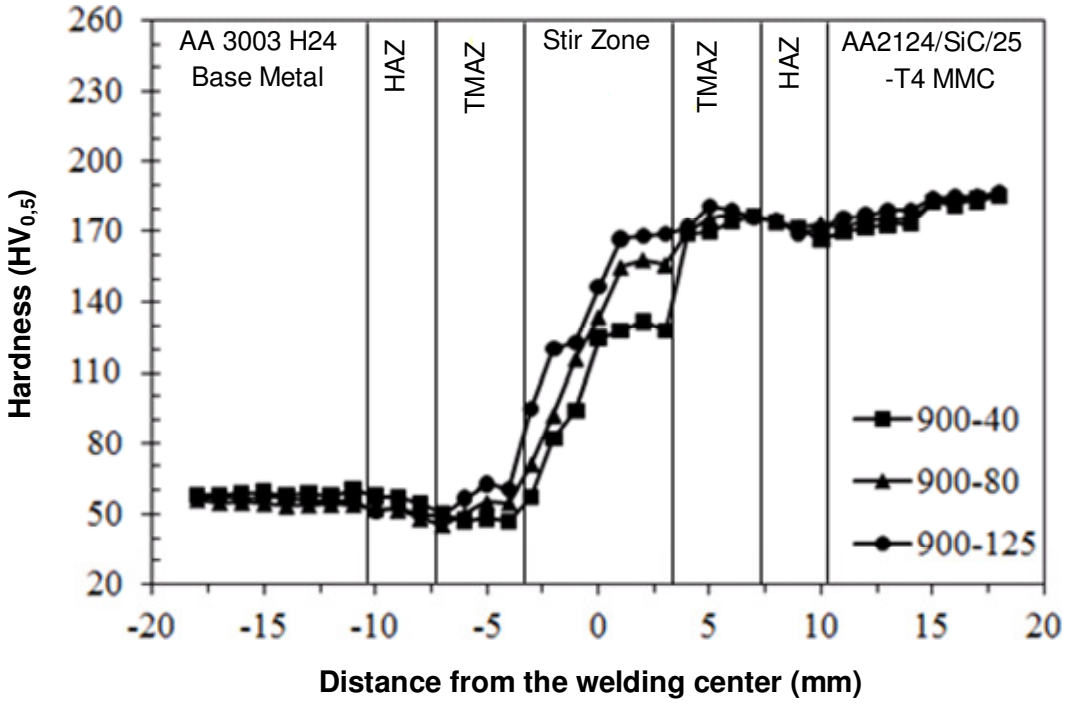

Figure 7. Microhardness profiles on the cross-section of the studied dissimilar joints at 900/40-125 welding parameters.

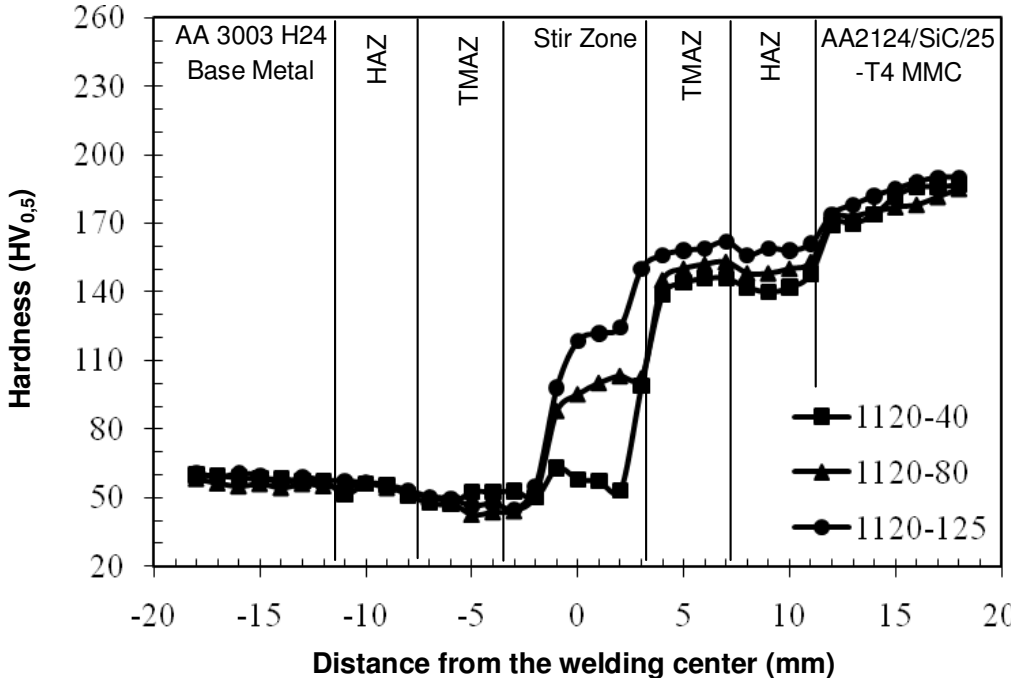

Figure 8. Microhardness profiles on the cross-section of the studied dissimilar joints at 1120/40-125 welding parameters.

in Figures 7 to 9. The microhardness values were in the range of 185 to 190 HV for AA2124/SiC/25p-T4 MMC and 55 to 60 HV for 3003-H24 Al alloy BM. All the microhardness profiles obtained from the joints exhibited

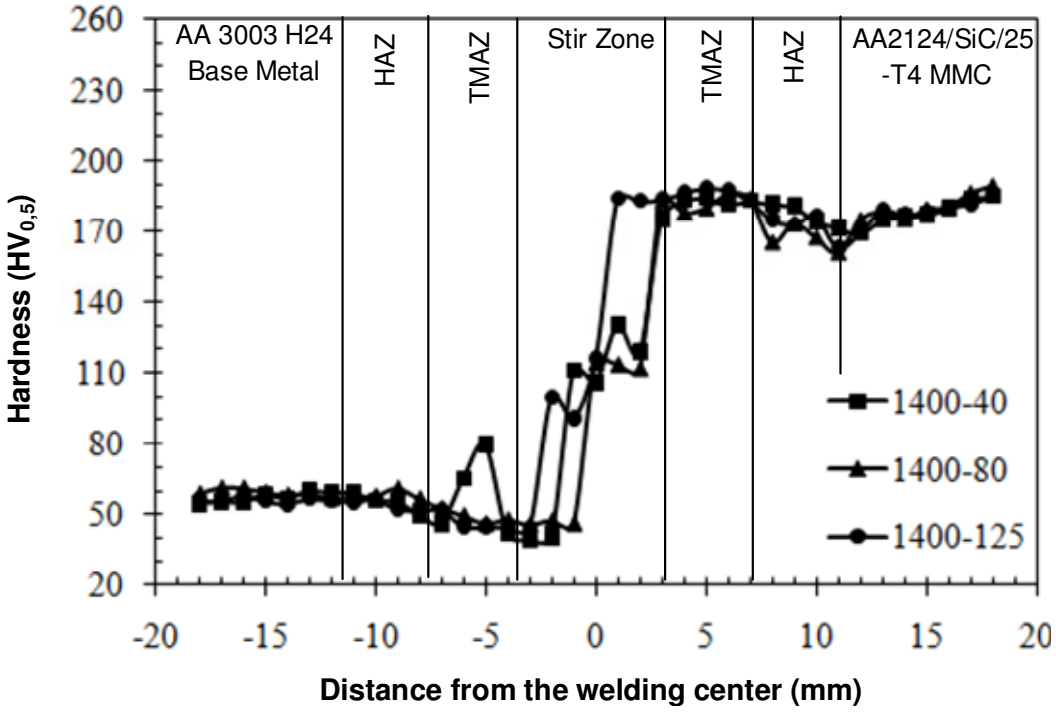

Figure 9. Microhardness profiles on the cross-section of the studied dissimilar joints at 1400/40-125 welding parameters.

a lower hardness value in the stir zone in comparison to MMC base material because of differences in the thermal expansion between Aluminum and MMC alloys rapid heating and cooling will give rise to the generation of dislocations at the matrix-SiC interface (Bozkurt et al., 2011a). The hardness decrease from the base material to the FSW zone was also observed in the unreinforced 6061 aluminium alloy, even if with a grain refinement of the aluminium alloy matrix (Liu et al., 1997). The refinement of the SiC particles and the grains contributed to the increase up to 170 HV in the hardness at the retreating side and 70 HV at the advancing side of the stir zone (Figure 7). The hardness values at the retreating side of the weld was also determined for the similar FSW joints of MMCs (Bozkurt et al., 2011a). The maximum hardness value was obtained in the joints produced at the traverse speed of 125 mm/min and tool rotation rates of 900-1400 rpm as shown in Figures 7 to 9. In all the conditions, the minimum hardness value is measured at the retreating side of the HAZ region due to the differences in the dislocation density (Storjohann et al., 2005), accelerated ageing and recovering processes caused by the weld thermal cycle as reported by Threadgill (1997) and an annealing effect (Cavaliere et al., 2009a). This is because of the fact that the HAZ region has been deformed very slightly, and has different thermo-mechanical behaviour with respect to the stir zone and the TMAZ. Some researchers showed such effect by analyzing the reinforcing particles behaviour about dimension and aspect ratio in the FSW Al alloy (Cavaliere et al., 2009a).

The hardness at the advancing side (AA3003-H24 side) of the HAZ region is higher than TMAZ because of thermal softening and frictional heating in this region, with the except in sample produced with 1400/40 rev/mm welding parameter as shown in Figure 9. In the joints produced with this welding parameter, the hardness increased up to 80 HV at the advancing side of the TMAZ region. This is attributed to the thermal effect, microstructural modifications and orientation of SiC particulates from stir zone to Al side (Figure 6b). The thermal effect and microstructural modifications occurring during the FSW joints depend on the different welding circumstances. (Sarsilmaz et al., 2010a; Cerri and Leo, 2010).

Tensile test results

The tensile test results and fracture locations of the dissimilar FSWed joints produced with different welding parameters are summarized in Table 2. Consistent and repetitive results were obtained from the tensile tests conducted. Most of the specimens extracted from the joints produced with the 900/40-80 and 1120-1400/80-125 welding parameters fractured in the HAZ region of AA3003-H24 side and the others fractured within the BM of AA3003-H24, except the joint obtained with 1400/40

Table 2. Tensile test results and fracture locations of the dissimilar FSWed joints.

Welding parameter		Ultimate tensile strength (MPa)	Elongation (%)	Joint efficiency (%)		Fracture zones
Tool rotation speed (rpm)	Tool traverse speed (mm/min)			According toAA2124/ SiCp/25-T4	According to AA3003 -H24	
AA2124/SiCp/25-T4 (BM)		453	1.4	-	-	-
AA3003-H24 (BM)		175	9.7	-	-	-
900	40	173	9.9	38.2	98.9	HAZ of AA3003-H24
900	80	175	10.4	38.8	100	HAZ of AA3003-H24
900	125	182	11,2	40.2	104	BM of AA3003-H24
1120	40	168	9.4	37.1	96	BM of AA3003-H24
1120	80	170	9.5	37.5	97.1	HAZ of AA3003-H24
1120	125	174	11	38.4	99.4	HAZ of AA3003-H24
1400	40	162	8.4	35.8	92.6	TMAZ of AA3003-H24
1400	80	167	9.4	36.9	95.4	HAZ of AA3003-H24
1400	125	171	10.6	37.8	97.7	HAZ of AA3003-H24

welding parameter, which is fractured along TMAZ of AA3003-H24 side. The fracture surfaces of the joints produced with 900/125 and 1400/40 welding parameters after the tensile testing are shown in Figures 10 and 11. The tensile strength and percent elongation values increased with the increasing tool transverse speeds at constant tool rotational speeds. The maximum tensile joint efficiency value was obtained from the joint produced at 900/125 welding parameters, that is 104% (that is $UTS_{FSW}/UTS_{base\ material}$ x 100), which was higher than the tensile strength of AA3003-H24 BM but much lower than MMC (40.2%). On the other hand, the elongation value of this joint was higher than both base plates especially MMC. The lowest tensile joint efficiency and percent elongation values were obtained from the joint produced with 1400/40 welding parameters. The tool transverse speed had a strong effect on the weldability of FSWed dissimilar alloys. The softened area was narrower for the high tool transverse speed than for the lower tool transverse speed. Thus, the strength of joints is strongly affected by transverse speed as the case for simmilar MMC joints (Sarsilmaz et al., 2010a). So, it can be concluded that the welding parameters are very influential on the joining efficiency. The reasons for obtaining different joint efficiency values for the Al/MMC dissimilar joints are obviously complex. One of the reasons is the different peak temperatures the material experiences during FSW as a result of various welding parameters. Another reason is the temper condition, that is aged (Bozkurt et al., 2009) or solution treated. The temper condition plays a significant effect on the mechanical behaviour of the joints (Çam and Koçak, 1998; Çam, 2011). It is well known that the reinforcement particles have a significant influence on the strength of the MMCs. Because of the SiC particulates non-uniform distributed at the TMAZ region of AA3003-H24 in this zone ultimate tensile strength and elongation is reduced down to 162 MPa and 8.4%, respectively.

Fracture surface analysis

The fracture surfaces of two dissimilar joints, one being with the highest joint efficiency and the other with the lowest joint efficiency, were examined using SEM micrographs to identify the fracture mechanisms as shown in Figures 9 and 10. Figures 12 and 13 also show different

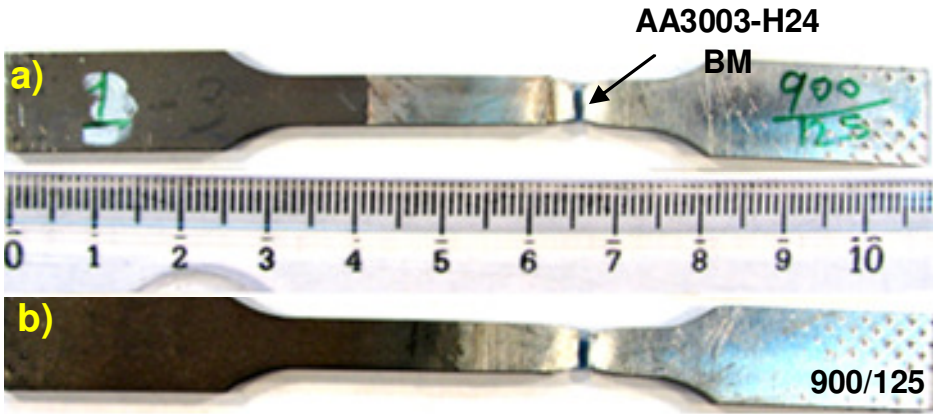

Figure 10. Fracture appearances after tensile tests of the FSWed dissimilar AA3003-H24 and AA2124/SiCp/25-T4 alloys at 900/125 welding parameters; a) upper and b) back side of the weld.

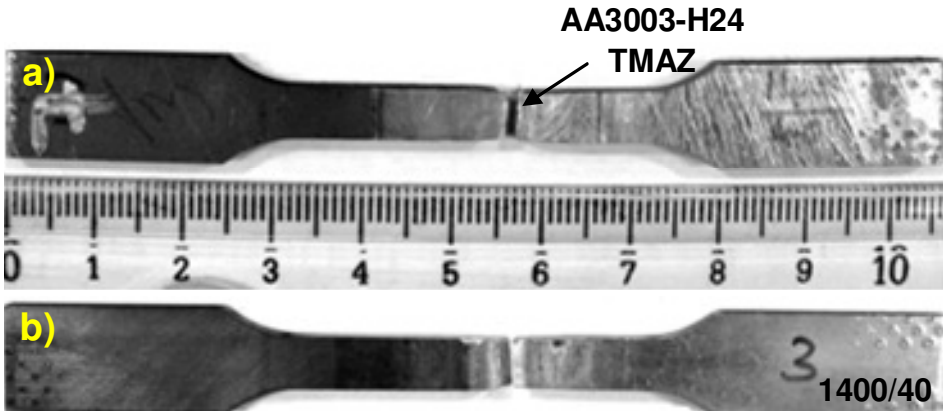

Figure 11. Fracture appearances after tensile tests of the FSWed dissimilar AA3003-H24 and AA2124/SiCp/25-T4 alloys at 1400/40 welding parameters; a) upper and b) back side of the weld.

magnifications of these fracture surfaces in these two samples. The results of EDS analysis conducted on the joints produced are also presented. SEM analysis results indicated that ductile fracture of the Al matrix took place, which had an excellent cohesion with the reinforcement particles (Ceschini et al., 2010). The specimens extracted from the joint with the highest joint efficiency exhibited a typical ductile mode of failure characterized by the presence of dimples known as microvoid coalescence. The specimens extracted from the joint with the lowest efficiency, on the other hand, displayed a mixed mode of fracture, consisting of ductile and brittle fracture, but generally brittle fracture.

Conclusions

The effect of the welding parameters on the microstructural and mechanical properties of FWSed dissimilar aluminium alloys joints was investigated in this study. The results obtained can be summarized as follows:

1) AA 3003 H24 and 2124/SiC/25-T4 dissimilar alloys plates were successfully joined by FSW without any visible superficial porosity or macroscopic defects on the top and bottom regions of welded samples, except the one produced with a traverse speed of 40 mm/min.
2) In the SEM examination, no evidence of porosity and article cracking or tool wear was observed in the stir zones of the welds.
3) All the microhardness profiles of the dissimilar Al/MMCs FSW joints exhibited a lower hardness in the stir zone. The hardness in the advancing side (AA3003-H24 Al side) of the HAZ region is higher than TMAZ because of thermal softening and frictional heating apart

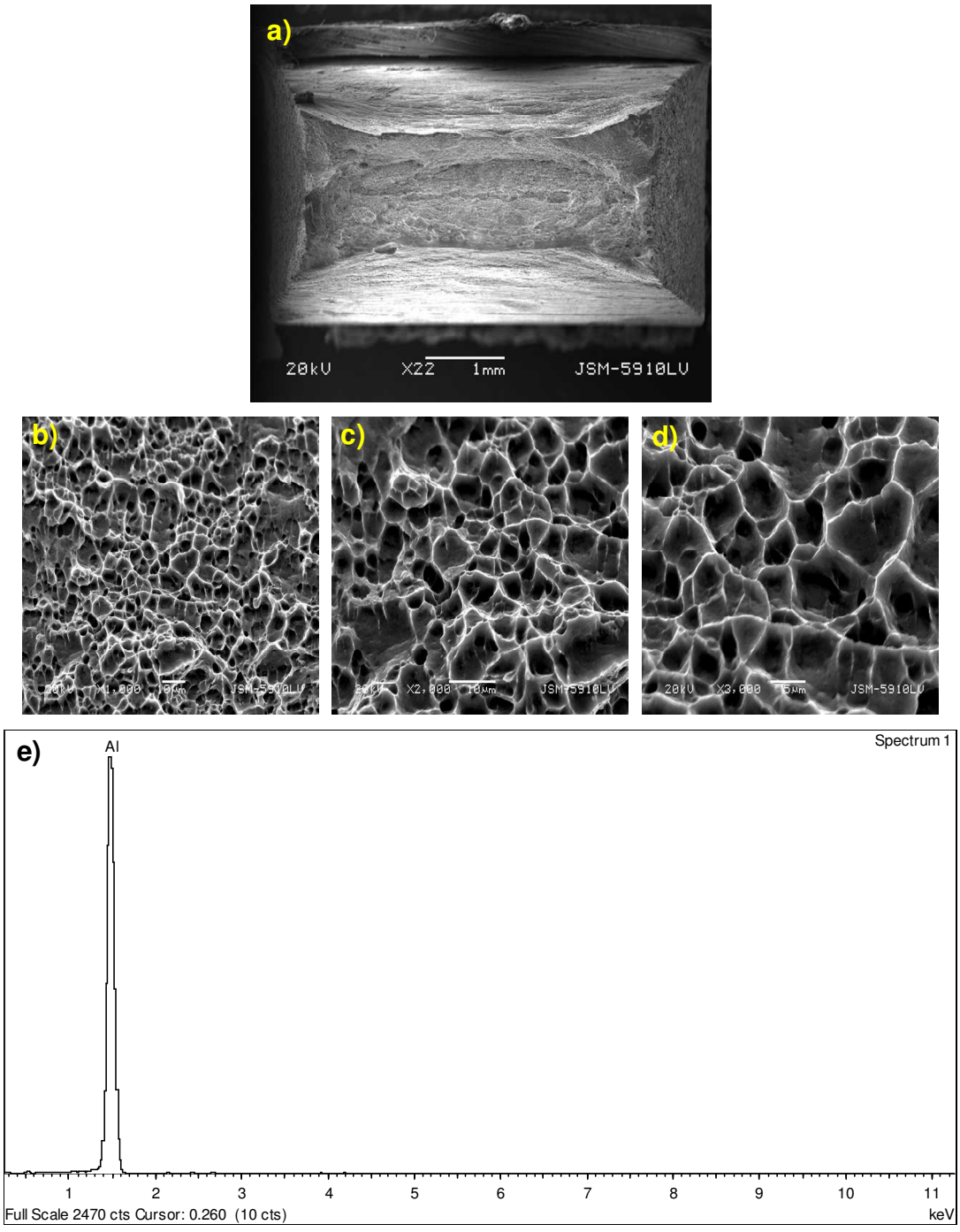

Figure 12. SEM micrographs and EDS analysis of the fracture surfaces of FSWed dissimilar Al/MMC alloys at 900/125 welding parameters after tensile test; a) 22X, b) 1000X, c) 2000X, d) 3000X and e) EDS analysis.

from the dissimilar Al/MMCs FSW joint produced with 1400/40 welding parameters. In this welding parameter, the hardness increased up to 80 HV at the advancing side of the TMAZ region and thus a weaker joint efficiency value was obtained.

4) Tensile test results indicated that high quality dissimilar Al/MMC joints could be obtained by FSW with 900/125 welding parameters.

5) The joint with the highest joint efficiency exhibited a typical ductile mode of failure. The joint with the lowest

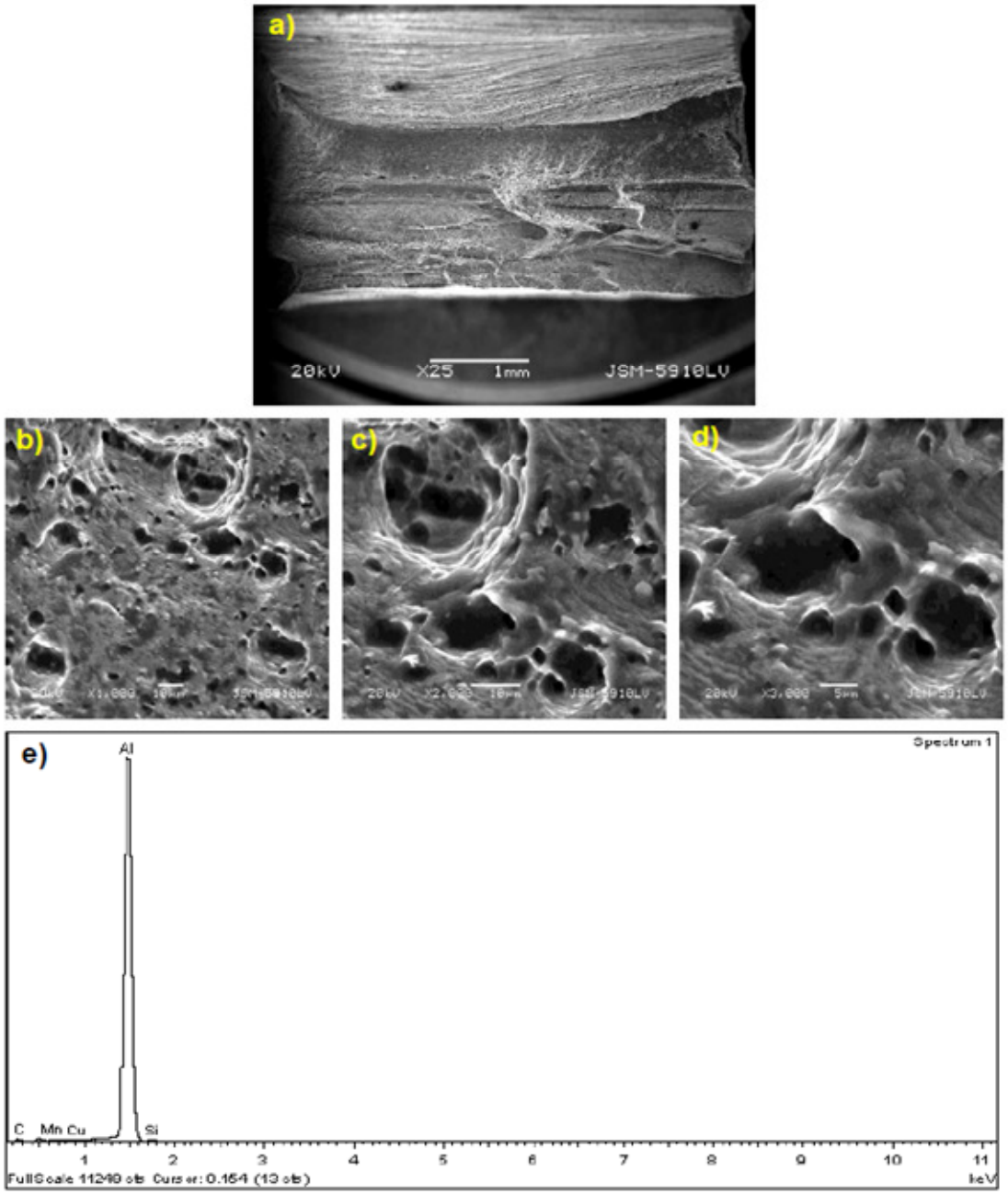

Welding parameter	Fracture zone	Kimyasal Element (%)				
1400/40	TMAZ of advancing side	C	Al	Si	Mn	Cu
		15.38	82.91	0.85	0.81	0.05

Figure 13. SEM micrographs and EDS analysis of the fracture surfaces of FSWed dissimilar Al/MMC alloys at 1400/40 welding parameters after tensile test; a) 22X, b) 1000X, c) 2000X, d) 3000X and e) EDS analysis.

joint efficiency, on the other hand, displayed a mixed mode fracture containing both ductile and brittle fracture, but generally brittle.

ACKNOWLEDGEMENTS

The authors are deeply grateful for the financial support of Marmara University Scientific Research Fund (BAPKO), Grant No: FEN-C-YLP-280110-0012. The authors also wish to Express their thanks to Ph.D.Murat DUNDAR of ASSAN (TR) for his assistance in supplying the aluminum sheets.

REFERENCES

ASTM E3-01 (2007). Standard practice for preparation of metallographic specimens. ASM international.

Barlas Z**,** Uzun H (2010). Microstructure and mechanical properties of friction stir butt welded dissimilar pure copper/brass alloy plates. Int. J. Mat. Res. (Z.Metallkd.). 101(6): 801-807.

Bozkurt Y, Uzun H, Salman S (2011a). Microstructure and mechanical properties of friction stir welded particulate reinforced AA2124/SiC/25p-T4 composite. J. Comp. Mat. DOI: 10.1177/0021998311401067.

Bozkurt Y, Uzun H, Salman S (2011b). The effect of tool wear on mechanical properties of friction stir welded AA2124/SiCp/25 composite plates. J. Fac. Eng. Arch., 26(1): 139-149.

Bozkurt Y, Artir R, Uzun H, Salman S (2009). Effect of subsequent aging in SiC_p reinforced AA2124 aluminum metal matrix composite. Adv. Comp. Lett., 18(5):151-155.

Çam G and Koçak M (1998). Joining of metal matrix composites and joining of other advanced materials. Progress in Joining of Advanced Materials - Part II: Sci. Tech. Weld. Joining., 3(4): 159-175.

Çam G, Ventzke V, Dos Santos JF, Koçak M, Jennequın G, Gonthıer-Maurın P (1999). Characterisation of electron beam welded aluminium alloys. Sci. Tech. Weld. Joining., 4(5): 317-323.

Çam G, Ventzke V, Dos Santos JF, Koçak M, Jennequın G, Gonthıer-Maurın P, Penasa M, Rivela C, Boisslier D (2000). Characterization of laser and electron beam welded Al-alloys. Pract. Metallography, 37(2): 59-89.

Çam G and Koçak M (2007). Microstructural and mechanical characterization of electron beam welded Al-alloy 7020. J. Mater. Sci., 42(17): 7154-7161.

Çam G (2011). Friction stir welded structural materials beyond Al-alloys. Int. Mat. Rev. 56(1): 1-48.

Cavaliere P, Santis AD, Panella F, Squillace A (2009a). Effect of welding parameters on mechanical and microstructural properties of dissimilar AA6082-AA2024 joints produced by friction stir welding. Mat. and Design., 30: 609-616.

Cerri E, Leo P (2010). Warm and room temperature deformation of friction stir welded thin aluminium sheets. Mat. Design., 31: 1392-1402.

Ceschini L**,** Morri A, Rotundo F, Jun TS, Korsunsky AM (2010). A study on similar and dissimilar linear friction welds of 2024 Al alloy and 2124Al/SiC_p composite. Adv. Mat. Res., 89-91: 461-466.

Ceschini L, Boromei I, Minak G, Morri A, Tarterini F (2007a).

Microstructure, tensile and fatigue properties of AA6061/20vol.%Al_2O_{3p} friction stir welded joints. Composites A, 38: 1200-1210.

Ceschini L, Boromei I, Minak G, Morri A, Tarterini F (2007b). Effect of friction stir welding on microstructure, tensile and fatigue properties of the AA7005/10 vol.%Al_2O_{3p} composite. Compos. Sci. Technol., 67: 605-615

Chen CM, Kovacevic R (2004). Joining of Al 6061 alloy to AISI 1018 steel by combined effects of fusion and solid state welding. Int. J. Mach. Tools Man., 44: 1205-1214.

Feng AH, Xiao BL, Ma ZY (2008). Effect of microstructural evolution on mechanical properties of friction stir welded AA2009/SiC composite. Comput Sci Technol., 68: 2141-2148.

Ghosh M, Kumar K, Kailas SV, Ray AK (2010). Optimization of friction stir welding parameters for dissimilar aluminum alloys. Mat. Design., 31: 3033-3037.

Gopalakrishnan S and Murugan N (2011). Prediction of tensile strength of friction stir welded aluminium matrix TiCp particulate reinforced composite. Mat. Design., 32: 462-467.

ISO/TTA2 (1997). Tensile tests for discontinuously reinforced metal matrix composites at ambiant temperatures. First edition. Techn. trends assess. pp. 4-15.

Khodir SA, Shibayanagi T (2008). Friction stir welding of dissimilar AA2024 and AA7075 aluminum alloys. Mat. Sci. Eng. B., 148: 82-87.

Leal RM, Loureir A (2008). Effect of overlapping friction stir welding passes in the quality of welds of aluminium alloys. Mat. Design., 29(5): 982–991.

Lee WB, Yeon YM and Jung SB (2003). The joint properties of dissimilar formed Al alloys by friction stir welding according to the fixed location of materials. Scripta Materll., 49: 423-428.

Liu C, Chen DL, Bhole S, Cao X, Jahazi M (2009). Polishing-assisted galvanic corrosion in the dissimilar friction stir welded joint of AZ31 magnesium alloy to 2024 aluminum alloy. Mater. Charac., 60: 370-376.

Liu P, Shi Q, Wang W, Wang X, Zhang Z (2008). Microstructure and XRD analysis of FSW joints for copper T2/aluminium 5A06 dissimilar materials. Mat. Lett., 62: 4106-4108.

Liu G, Murr LE, Niou CS, McClure JC, Vega FR (1997). Microstructural aspects of the friction-stir welding of 6061-T6 aluminum. Scripta Materll, 37: 355-361.

Mei-jun Z, Dong-yan D, Yong-jin G, Guo-zhen C, Ming L, Da-li M (2010). Effect of Zn content on tensile and electrochemical properties of 3003 Al alloy. Trans. Nonferr. Met. Soc. Ch. 20: 2118-2123.

Najafabadi MF, Kashani-Bozorg SF, Hanzaki AZ (2010). Joining of CP-Ti to 304 stainless steel using friction stir welding technique. Mat. Design., 31(10): 4800-4807.

Nami H, Adgi H, Sharifitabar M, Shamabadi H (2011). Microstructure and mechanical properties of friction stir welded Al/Mg_2Si metal matrix cast composite. Mat. Design., 32: 976-983.

Rotundo F, Ceschini L, Morri A, Jun TS, Korsunsky AM (2010). Mechanical and microstructural characterization of 2124Al/25vol%SiC_p joints obtained by linear friction welding (LFW). Composites A, 41:1028-1037.

Sarsilmaz F, Çaydaş U, Hasçalik A, Tanriover L (2010a). The joint properties of dissimilar aluminum plates joined by friction stir welding. Int. J. Mat. Res., 101: 692-699.

Shanmuga SN, Murugan N (2010) Tensile behavior of dissimilar friction stir welded joints of aluminium alloys. Mat. Design., 31: 4184-4193.

Sharifitabar M, Nami H. Microstructures of dissimilar friction stir welded joint between 2024-T4 aluminum alloy and Al/Mg_2Si metal matrix composite, Composite part B, Doi: 10.1016/j.compositesb.2011.05.025.

Shigematsu I, Kwon YJ, Suzuki K, Imai T, Saito N (2003). Joining of 5083 and 6061 aluminum alloys by friction stir welding. J. Mater. Sci. Lett., 22: 353-356.

Somasekharan AC, Murr LE (2004). Microstructures in friction-stir welded dissimilar magnesium alloys and magnesium alloys to 6061-T6 aluminum alloy. Mat. Charc., 52: 49-64.

Storjohann D, Barabash OM, Babu SS, David SA (2005). Fusion and Friction Stir Welding of Aluminum-Metal-Matrix Composites. Met. Mat. Trans., 36A: 3237-3247.

Tanaka T, Morishige T, Hirata T (2009a). Comprehensive analysis of joint strength for dissimilar friction stir welds of mild steel to aluminum alloys. Scripta Materialia, 61: 756-759.

Threadgill P (1997). Friction stir welds in aluminium alloys-preliminary microstructural assessment. Industrial Report 513/2/97 of The Welding Institute-TWI.

Uzun H (2007). Friction stir welding of SiC particulate reinforced AA2124 aluminium alloy matrix composite. Mat. Design., 28: 1440-1446.

Uzun H, Done CD, Argagnotto A, Ghidini T, Gambaro C (2005). Friction stir welding of dissimilar Al 6013-T4 to X5CrNi18-10 stainless steel. Mat. Design., 26: 41-46.

Wert JA (2003). Microstructures of friction stir weld joints between an aluminum base metal matrix composite and a monolithic aluminum alloy. Scripta Materll, 49: 607-612.

Xue P, Xiao BL, Ni DR, Ma ZY (2010). Enhanced mechanical properties of friction stir welded dissimilar Al–Cu joint by intermetallic compounds. Mat. Sci. Eng. A., 527: 5723-5727.

Yong Y, Da-tong Z, Cheng Q, Wen Z (2010). Dissimilar friction stir welding between 5052 aluminum alloy and AZ31 magnesium alloy. Trans. Non. Met. Soc. China., 20: 619-623.